Journal of Neuroscience Research

JNR

Volume 91 Number 3 March 2013

Published online 27 November, 2012 – 30 December, 2012

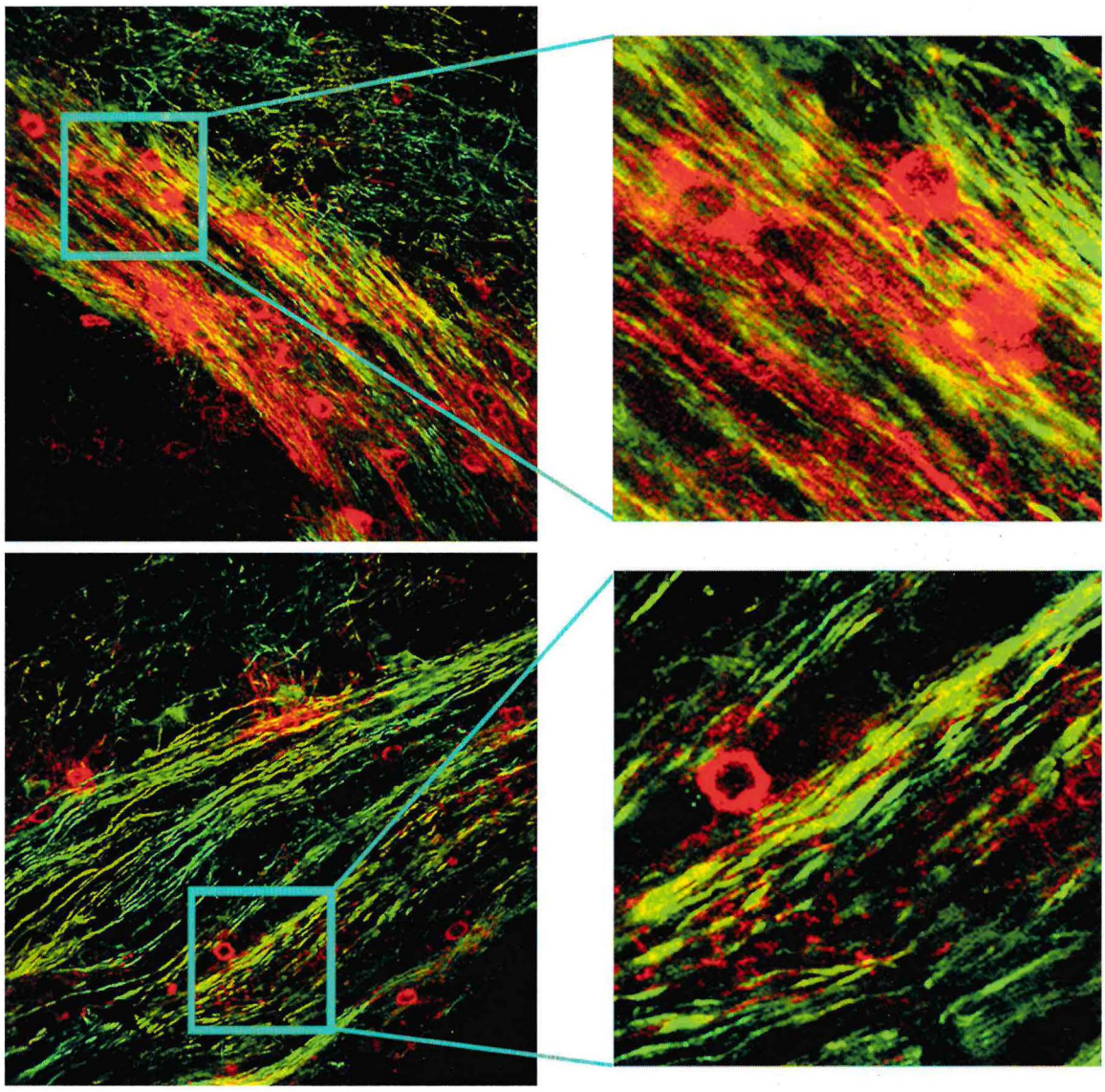

WILEY-BLACKWELL

ISSN 0360-4012

Journal of Neuroscience Research

Journal of Neuroscience Research 91:335–348 (2013)

A DEAD-Box RNA Helicase Ddx54 Protein in Oligodendrocytes Is Indispensable for Myelination in the Central Nervous System

Rui Zhan,[1] Masahiro Yamamoto,[1,2]* Toshiyuki Ueki,[2] Nozomu Yoshioka,[3] Kayoko Tanaka,[4] Hiromi Morisaki,[5] Chika Seiwa,[1] Yuta Yamamoto,[6] Hitoshi Kawano,[3] Yoshihiro Tsuruo,[6] Kenji Watanabe,[1] Hiroaki Asou,[1] and Sadakazu Aiso[1]*

[1]Center for Kampo Medicine, Keio University School of Medicine, Tokyo, Japan
[2]Tsumura Research Laboratories, Tsumura and Co., Ibaraki, Japan
[3]Department of Brain Development and Neural Regeneration, Tokyo Metropolitan Institute of Medical Science, Tokyo, Japan
[4]Biomedical Research Center, Division of Morphological Science, Saitama Medical School, Saitama, Japan
[5]Central Research Laboratories, Sysmex Corporation, Kobe, Japan
[6]Department of Anatomy and Cell Biology, Wakayama Medical University School of Medicine, Wakayama, Japan

We recently reported that a new monoclonal antibody, 4F2, which labels oligodendroglial lineage cells, recognizes a DEAD-box RNA helicase Ddx54 and that Ddx54 binds to myelin basic protein (MBP) in brain and cultured oligodendrocytes. To elucidate the biological function of Ddx54, we generated a recombinant adenovirus, Ad-shRNA:Ddx54, expressing a short hairpin RNA to silence endogenous Ddx54 protein. The virus was intraventricularly injected into the brains of mice on postnatal day (PD) 2. The brains at PD 9 were then analyzed by immunohistochemistry. In untreated normal brain sections, as well as control brains that had been injected with Ad-β-Gal, myelination of axons occurred in the corpus callosum with filamentous patterns of immunosignals of myelin-associated glycoprotein (MAG) and MBP. In Ad-shRNA:Ddx54-injected brain, substantial amounts of MAG and MBP immunosignals were present, but MBP immunosignals accumulated in the subplate layer and did not intrude into the emerging white matter. Immunoblot analysis revealed that Ddx54 knockdown caused a significant decrease in the level of 21.5 kDa MBP isoform and Ddx54, but the amount of Olig2; 2′,3′-cyclic nucleotide 3′ phosphodiesterase; MAG; three MBP isoforms (14, 17.5, and 18 kDa); and QKI-5, QKI-6, and QKI-7 proteins remained unchanged. Transfection of the Ddx54 expression vector into luciferase reporter-introduced neuroepithelial cells resulted in upregulated MBP promoter activity. Immunoprecipitation of Ddx54 protein in MBP-transfected HEK293 cells indicated that Ddx54 may directly interact with MBP mRNA. These results suggest that Ddx54 protein play an important role in central nervous system myelination, presumably in myelin sheath formation after the differentiation of oligodendrocytes.

Key words: myelin basic protein; myelin-associated glycoprotein; adenoviral vector; RNA interference

Oligodendrocytes are responsible for myelination in the central nervous system (CNS). The oligodendrocyte precursor cells (OPCs) are derived from pluripotent neural stem cells in the developing brain. The maturation of OPCs into myelin forming oligodendrocytes is characterized by the extension of numerous branched processes and membrane sheets along with the expression of myelin-specific proteins (Pfeiffer et al., 1993). Adequate OPC proliferation ensures the generation of a sufficient number of myelin-forming cells, and subsequent differentiation is a critical prerequisite for myelinating processes. Thus transition of OPCs from proliferation to differentiation is a key step that governs myelination (Dugas et al., 2007). However, the accumu-

Contract grant sponsor: Ministry of Education, Culture, Sports, Science and Technology of Japan; Contract grant number: 20500348(to H.A).

*Correspondence to: Masahiro Yamamoto, PhD, Tsumura Research Laboratories, Tsumura and Co., Yoshiwara 3586, Ami-machi, Inashiki-gun, Ibaraki 300-1192, Japan. E-mail: hirokoma@h.email.ne.jp or Sadakazu Aiso, M.D., Ph.D. Center for Kampo Medicine, Keio University School of Medicine, Tokyo, Japan. E-mail: aiso@a3.keio.jp

Requests for materials should be addressed to M. Yamamoto (hirokoma@h.email.ne.jp) or H. Asou (asou@a8.keio.jp).

Received 26 May 2012; Revised 22 September 2012; Accepted 2 October 2012

Published online 14 December 2012 in Wiley Online Library (wileyonlinelibrary.com). DOI: 10.1002/jnr.23162

lation of OPCs and their exit from the cell cycle are not sufficient for inducing OPC differentiation, maturation, and myelin sheath formation. Accordingly, in demyelinating diseases such as multiple sclerosis and progressive multifocal leukoencephalopathy, in spite of the accumulation of large numbers of OPCs in demyelinated lesions (Wolswijk, 1998), the OPCs fail to differentiate to mature oligodendrocytes and to myelinate axons (Piaton et al., 2009; Watzlawik et al., 2010). Thus, additional unknown mechanisms must directly regulate myelin sheath formation. We have recently reported that a new monoclonal antibody, 4F2 (Ueki et al., 2012), consistently and specifically labels a large portion of oligodendroglial cells appearing from the earliest stages of development (E9, in neuroepithelial cells of the rat neural tubes) to adult age (oligodendrocytes in 11-week-old brains). Specific staining by the antibody was demonstrated in OPC and oligodendrocyte cultures as well as in mouse and rat samples. Furthermore, the 4F2 antigen is thought to associate with myelin basic protein (MBP) isoforms in the brain and cultured oligodendrocytes. The antigen was identified as Ddx54, a DEAD-box RNA helicase, and cotransfection of the Ddx54 gene with MBP genes resulted in the altered nuclear localization of the 21.5-kDa MBP isoform. These findings suggest a possible role for Ddx54 in oligodendrocyte function. Until now, the biological activity of Ddx54 protein has not been reported, except for human DDX54, also known as DP97, which interacts with estrogen receptors (ERs) and represses the transcription of ER-regulated genes (Rajendran et al., 2003). In recent years, RNA interference (RNAi) has offered a powerful approach for targeted gene silencing by forming a complementary double-stranded RNA species in the sequence of interest. RNAi induction by short hairpin RNA (shRNA) or small interfering RNA (siRNA) transfection is the most time-efficient method for gene knockdown in mammalian cells (Alexander et al., 2007). Furthermore, gene transduction by a replication-deficient adenoviral vector has provided us with an effective means to manipulate specific genes in a broad range of cell types of various tissues, including the brain, for an extended period in vivo (Peltekian et al., 1997). In the present study, to elucidate the biological function of Ddx54 protein, we used intraventricular injection of the adenoviral vector expressing shRNA to silence Ddx54 protein. We found that knockdown of Ddx54 resulted in the extensive absence of MBP in the corpus callosum in spite of the presence of a large number of $Olig2^+$ OPCs and myelin-associated glycoprotein (MAG)-positive oligodendrocytes. Detailed analyses suggest a crucial role for Ddx54 protein in the final step of myelin sheath formation.

MATERIALS AND METHODS

DNA Constructs

Full-length cDNAs encoding Ddx54 and MBP were obtained from the RIKEN Fantom Clone (RIKEN Gnomic Science Center, Yokohama, Japan) and subcloned into pCMV-FLAG (Stratagene, Santa Clara, CA) and pCMV-Myc (Clontech, Mountain View, CA) vectors, respectively, as described previously (Ueki et al., 2012). A reporter plasmid pMBP-Luc was obtained by inserting 400 base pairs (bp) of the 5′-promoter region of mouse MBP (Miura et al., 1989) into the KpnI/HindIII site of pTAL-Luc vector (Clontech). Another reporter plasmid, pMBP-Luc-3UTR, was obtained by inserting the 3′-untranslated region (300 bp, amplified from RIKEN Fantom Clone) downstream of the luciferase gene of pMBP-Luc.

shRNA and Adenoviral Vector

The nucleotide sequences of mouse Ddx54 siRNAs were designed by Clontech. Based on the two nucleotide sequences for siRNA, eight shRNA sequences with some mutations were carefully designed to adapt the cloning cassettes and avoid unwanted homologous recombination events (see Fig. 1A). The sequences were cloned into two vectors, piGENE tRNA and pSilencer 1.0-U6 (Clontech). Next, we transfected these constructs into HEK293 cells (>80% transfection efficiency) and evaluated the silencing efficiency by PCR. We selected the piGENE m4F2-2L for adenoviral vector generation. The expression cassettes of piGENE m4F2-2 and *Escherichia coli* β-galactosidase LacZ gene were recloned into AdRGD vector to obtain pAd-shRNA:Ddx54 and the control vector pAd-β-Gal, respectively. Adenoviral vectors were prepared by GenoFunction Inc. (Tsukuba, Ibaraki, Japan).

Antibodies

Anti-Ddx54 mouse monoclonal antibody 4F2 (1:200; Ueki et al., 2012), anti-Camsap1 mouse monoclonal antibody A3B10 (1:200; Yamamoto et al., 2009; Yoshioka et al., 2011a), and anti-MBP rabbit polyclonal antibody (1:500; Akiyama et al., 2002) were prepared in our laboratory. Anti-MAG (1:3,000, rabbit polyclonal) and antineurofilament 145 kDa (1:200, rabbit polyclonal) antibodies were kindly provided by Dr. Y. Matsuda, National Center for Neurology and Psychiatry (Tokyo, Japan) and Dr. Y. Takahashi, Niigata University (Niigata, Japan), respectively. Anti-Olig2 (1:200, goat polyclonal; R&D Systems, Minneapolis, MN), antineurofilament 200 kDa (1:200, clone RT97, mouse monoclonal; Boehringer Mannheim Biochemicals, Indianapolis, IN), anti-Sox10 (1:200, goat polyclonal; Santa Cruz Biotechnology, Santa Cruz, CA), anti-CNPase (1:1,000, clone 11-5B, mouse monoclonal; Promega, Madison, WI), anti-MBP (1:200, clone MAB 387, mouse monoclonal; Chemicon/Millipore, Billerica, MA), anti-QKI-5 (1:500, rabbit polyclonal; Millipore), anti-QKI-6 (1:500, rabbit polyclonal; Millipore), anti-QKI-7 (1:500, rabbit polyclonal; Millipore), and antiactin (1:1,000, clone name C4, mouse monoclonal; Chemicon/Millipore) were also used.

Animals

Pregnant female C57BL/6 mice were purchased from Japan SLC (Shizuoka, Japan). The experimental protocol was approved by the Ethics Committee for Care and Use of Laboratory Animals for Biomedical Research of Tsumura Research Laboratories (Ami, Ibaraki, Japan).

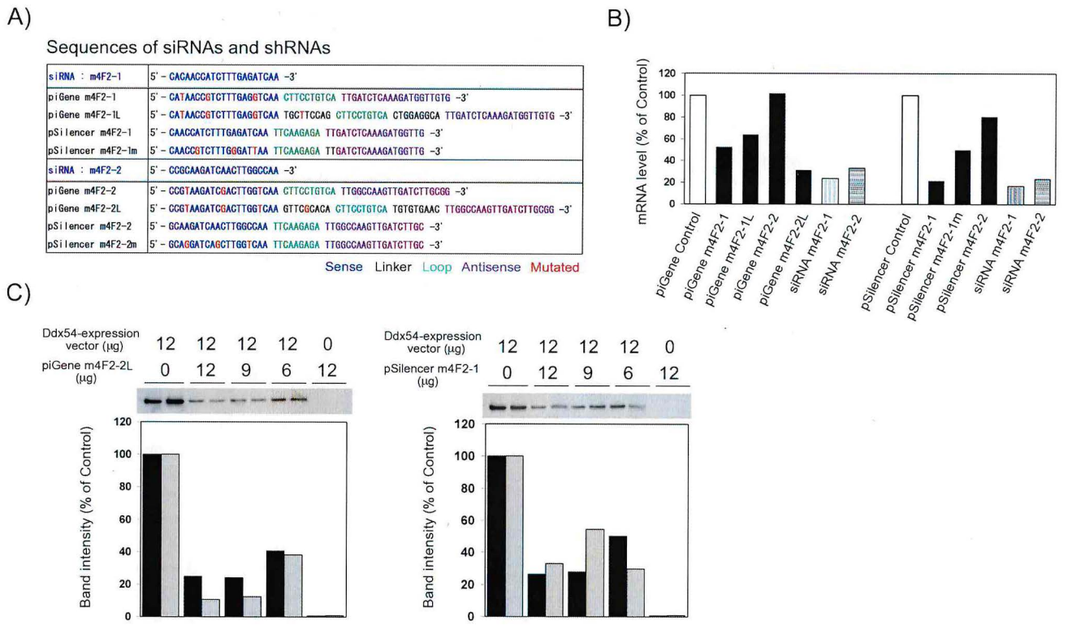

Fig. 1. Design of siRNA and shRNA for silencing Ddx54 and verification of its knockdown efficiency. **A:** Based on the two nucleotide sequences for siRNA, eight shRNA sequences were designed that included some mutations to 1) adapt for cloning cassettes and 2) avoid unwanted homologous recombination events. Sense (blue) and antisense (purple) sequences of siRNA and the sequences of the loop (green) and linker (black) are shown. The mutated nucleotides are highlighted in red. **B:** The sequences were cloned into two vectors, piGENE tRNA and pSilencer 1.0-U6, and the resultant 10 plasmids (containing two control plasmids) and two siRNAs were cotransfected with the Ddx54 expression vector into HEK293 cells. RT-PCR analysis was then performed on these cells to quantify the amount of Ddx54 mRNA. These data were used to establish the knockdown efficiency of the siRNAs and shRNA plasmids. No clone was obtained for pSilencer m4F2-2 transfection. The expression level was normalized to that of 18S rRNA and the relative ratio to the amount of Ddx54 mRNA in the control plasmid-transfected cells. **C:** The dose-responsive effect of piGene m4F2-2L and pSilencer m4F2-1 on the amount of Ddx54 protein was studied by immunoblot analysis. A 12-μg aliquot of Ddx54-expressing vector and 6–12 μg of knockdown vector at the amount indicated in the graph were cotransfected into HEK293 cells. The cells were then cultured for 24 hr. The cell lysate was analyzed by immunoblotting using anti-Flag tag antibody to detect Ddx54. The data are expressed as the relative ratio of the amount of Ddx54 protein in knockdown vector-transfected cells to that in the control plasmid-transfected cells (0 μg of either piGene m4F2-2L or piGene m4F2-1).

OPC Culture, Viral Infection, and Real-Time RT-PCR

OPCs were prepared from primary mixed cell cultures of embryonic mouse cerebral hemispheres as described previously (Imada et al., 2010). The purified OPCs were cultured for an additional 3 days and then infected with Ad-β-Gal or Ad-shRNA:Ddx54 adenoviruses. After 24 hr, total RNA was extracted from OPCs using an RNeasy kit (Qiagen, Valencia, CA) according to the manufacturer's instructions. Real time RT-PCR was performed by using a Taq-Man Gold RT-PCR Kit (Applied Biosystems, Foster City, CA) and an ABI Prism 7900 HT (Applied Biosystems).

Viral Injections

Five C57BL/6 mice 2 days after birth were anesthetized with ether and then positioned in a stereotaxic apparatus. A 2-μl aliquot of adenoviral solution (containing 6.0×10^6 ifu) was injected unilaterally (left side) through a 27-gauge needle attached to a Hamilton microsyringe in the dorsolateral portion of the lateral ventricle. The adjacent brain region is that in which most cells of the persisting subventricular zone (SVZ) are located in postnatal life (Goldman, 1995). After injection, the pups were revived by warming before being returned to their mothers. The survival rate was >98% with over 50 pups. The pups were sacrificed on postnatal day (PD) 5 and their brains processed for immunohistochemical and biochemical analyses. With this protocol, we found that over 80% of $Olig2^+$ cells were stained by X-gal.

Tissue Processing and Microscopic Observations

All the mice were deeply anesthetized with ether, perfused with 4% paraformaldehyde, and stored in a fixative solution containing 0.2% glutaraldehyde in 0.2 M phosphate buffer, pH 7.4. The cerebral hemispheres were separated in all cases

and sectioned serially in the coronal plane at 10 μm with a microtome. The coronal section was prepared from the locus suitable for presentation of each target molecule (for example, MAG for −1.22 mm Bregma and MBP for −2.30 mm Bregma). The same locus was prepared from both groups. However, because of the large volume of intraventricular injection solution and accompanying inflammation induced by injection of the virus, enlargement of the ventrical space was occasionally observed in some virus-injected brains. Nonetheless, this enlargement gave no discernible change in the distribution of immunosignals examined in the present study, at least at the level of light microscopic observations (unpublished data).

Immunohistochemistry

Immunohistochemistry was performed as previously described (Yoshioka et al., 2010, 2011b). Free-floating sections were initially rinsed in 20 mM phosphate-buffered saline (PBS) and incubated in a mixture of 3% hydrogen peroxide and 0.1% Triton X-100 for 15 min at room temperature. After rinsing in 20 mM PBS, the sections were incubated overnight at 4°C with the first antibody, which was diluted with 20 mM PBS-containing 0.5% skimmed milk. After rinsing in 20 mM PBS for 15 min, sections were incubated with biotinylated secondary antibody (1:100; Vector Laboratories, Burlingame, CA) for 30 min at 37°C. The sections were rinsed with 20 mM PBS for 15 min and then incubated in avidin-biotin peroxidase complex (Vectastain ABC kit; Vector Laboratories) for 30 min at 37°C. After rinsing with 20 mM PBS, immunoreaction was visualized in a solution containing 0.01% diaminobenzidine tetrahydrochloride and 0.01% hydrogen peroxide in 50 mM Tris buffer (pH 7.4) at 37°C for 5–10 min. Sections were mounted on MAS-coated glass slides (Matsunami Glass, Osaka, Japan), air dried on a hotplate at 40°C, and coverslipped with Entellan New (Merck, Darmstadt, Germany) after dehydration through ethanol and xylene. Digital images were taken with an AxioVision CCD system (Carl Zeiss, Göttingen, Germany), and the TIF files were processed in Adobe Photoshop (Adobe Systems, San Jose, CA). The intensity of immunosignals was measured (n = 3) using BZ-8100 BIOZERO measurement software (Keyence Coorporation, Osaka, Japan).

Immunofluorescent Staining

Free-floating sections were incubated in 20 mM PBS containing 0.1% Triton X-100 for 15 min at room temperature. After being rinsed with 20 mM PBS, sections were incubated overnight at 4°C with antibodies. For double-immunofluorescence staining, sections were incubated in mixtures of Alexa Fluor 488-conjugated secondary antibody (1:100; Molecular Probes, Eugene, OR) and biotinylated secondary antibody (1:100) for 60 min at 37°C. Sections were then incubated with streptavidin-Alexa Fluor 594 conjugate (1:100; Molecular Probes) for 60 min at 37°C. Mounted sections were air dried on a hotplate at 40°C and coverslipped. Sections were observed and digital images were recorded with a confocal laser scanning microscope (FV-1000; Olympus). Both brightness and background were adjusted to enhance the clarity of images. The intensity of immunosignals was measured (n = 3) using BZ-8100 BIOZERO measurement software, and the ratio of MAG or MBP to neurofilament was calculated.

Reporter Assay

Neuroepithelial cells from mouse fetuses were prepared and cultured as described previously (Nakashima et al., 1999). In brief, telencephalons from mice on E14 were triturated in Hanks' balanced salt solution by frequent pipetting, and dissociated cells were expanded for 4 days in N_2-supplemented DMEM/F12 medium (Life Technologies, Carlsbad, CA) containing 10 ng/ml of basic fibroblast growth factor (b-FGF; R&D Systems; N2/DMEM/F12/b-FGF) in 10-cm dishes that had been precoated with poly-L-ornithine (Sigma/Aldrich, St. Louis, MO) and fibronectin (Life Technologies). The cells were plated at 1×10^5 cells/well in 24-well plates precoated as described above. Sixteen hours after the passage, cells were transfected with 0.8 μg reporter plasmid, 0.2 μg Ddx54-expressing plasmid, and 0.04 μg *Renilla* luciferase-expressing plasmid (as an internal transfection efficiency control) by the Lipofectamine method, following the manufacturer's instructions (Life Technologies). Twenty-four hours after transfection, the cells were stimulated with 1 mM dibutyryl cAMP (dbcAMP) and 0.25 mM theophylline or 10 nM 17β-estradiol. The transfected cells were examined for firefly and *Renilla* luciferase activities using the Dual-Luciferase Reporter Assay system (Promega).

Ribonucleoprotein Immunoprecipitation Assay

Identification of *Mbp* mRNAs bound to Ddx54 protein was performed by ribonucleoprotein immunoprecipitation (RIP) assay using a Ribocluster Profiler kit (Medical and Biological Laboratories Co., Nagoya Aichi, Japan), according to the supplier's protocol. Briefly, HEK293 cells were cotransfected with pCMV-Ddx54-Flag and pCMV-MBP-Myc plasmids by Lipofectamine 2000 (Life Technologies). Twenty-four hours after transfection, cell lysate was immunoprecipitated with anti-Flag antibody-immobilized Dynabeads Protein G (Life Technologies), and RNA was isolated from the precipitate using guanidine hydrochloride. The RNA was analyzed by RT-PCR with the primers to *Mbp*, forward: 5′-ATGGCATCACAGAAGAGACCCTC-3′, reverse: 5′-TCAGCGTCTCGCCATGGGAGAT-3′. The PCR products were analyzed by agarose gel electrophoresis, and the images were obtained by using a Typhoon Imaging System (GE Healthcare, Little Chalfont, United Kingdom). As control experiments, PCR using primers specific for GAPDH, ubiquitin, and actin was also performed on the immunoprecipitated RNA and gave no band for these mRNA species (data not shown). RT-PCR in the absence of reverse transcriptase was also conducted to check for possible contamination of *Mbp* DNA from pCMV-MBP-Myc plasmid.

Statistical Analysis

Data are shown as mean ± SD of three independent experiments. Differences between groups were analyzed by *t*-test with Bonferroni correction for multiple comparisons. $P < 0.05$ was considered significant.

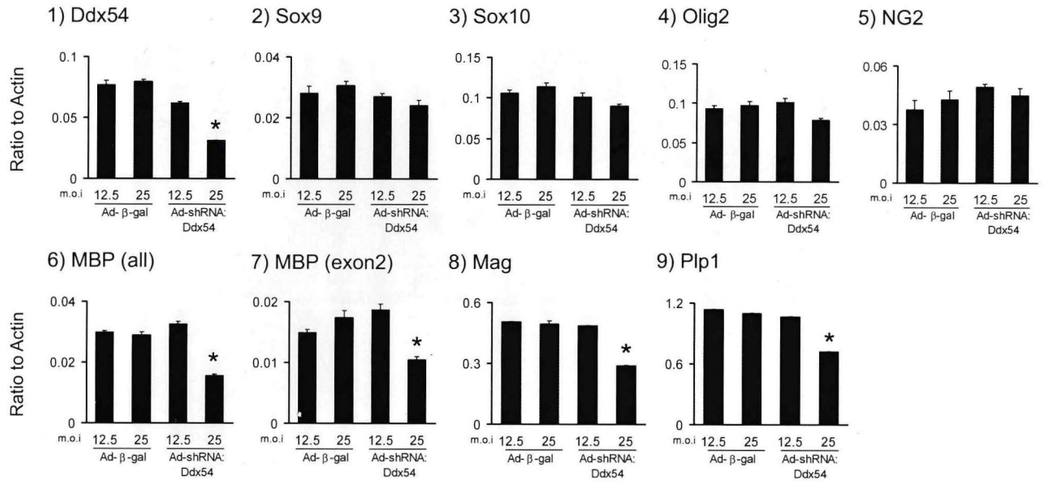

Fig. 2. Effect of Ad-shRNA:Ddx54 infection on gene expression in the cultured OPCs. In-vitro-cultured OPCs were infected with Ad-β-Gal or Ad-shRNA:Ddx54 at moi indicated in the graph. The cells were further incubated for 24 hr, and the gene expression of Ddx54, Sox9, Sox10, Olig2, NG2 (Cspg4), Mbp, Mag, and Plp-1 was analyzed by quantitative real-time RT-PCR. The expression of Mbp was assessed by two types of primer/probe sets; i.e., one is specific for all four isoforms [Mbp(all)] and the other for the 17- and 21.5-kDa isoforms [Mbp(exon 2)] only. Data represent mean ± SEM (n = 3). *$P < 0.05$ vs. Ad-β-Gal-infected cells at equal moi.

RESULTS

Generation of Recombinant Adenovirus

We selected two nucleotide sequences for siRNA that showed about 80% knockdown efficiency of Ddx54 by transfection with Lipofectamine 2000. Eight nucleotide sequences were designed that included mutations in order to adapt the cloning cassettes and to avoid unwanted homologous recombination events. The sequences were cloned into two vectors, piGENE tRNA and pSilencer 1.0-U6 (Fig. 1A). Fourteen different plasmids were obtained and transfected into HEK293 cells with Flag-tagged Ddx54-expressing vector. The mRNA levels of 4F2 after 24 hr were measured. Approximately 80% knockdown efficiency was obtained using piGene m4F2-2L and pSilencer m4F2-1 (Fig. 1B). The Ddx54 protein level was evaluated by immunoprecipitation with anti-Flag tag antibody, and both plasmids decreased Ddx54 protein repeatedly in a dose-dependent manner (Fig. 1C). We then recloned the expression cassette of piGene m4F2-2L into pAdHM15RGD and generated Ad-shRNA:Ddx54 adenovirus using this plasmid. In vitro cultured OPCs were infected with Ad-shRNA:Ddx54 and an adenovirus vector encoding the *Escherichia coli* β-galactosidase gene LacZ (Ad-β-Gal), and expression of Ddx54 mRNA was evaluated by RT-PCR. As shown in Figure 2, Ad-shRNA:Ddx54 dose dependently decreased Ddx54 mRNA expression, indicating that the viral vector works well in OPCs. The mRNA expression of other oligodendroglial markers was also examined (Fig. 2). Our results demonstrate that the expression levels of Mbp, Mag, and Plp1 also decreased and that those of Sox9, Sox10, Olig2, and NG2 showed no significant change. The expression of MBP was assessed by two types of primer/probe sets, i.e., one specific for all four isoforms and the other for the 17 and 21.5-kDa isoforms, and both gave similar results.

Intraventricular Administration of shRNA-Ddx54-Expressing Adenoviral Vector Into the Brain of Neonatal Mice

First, we injected a control adenovirus (Ad-β-Gal) into the left lateral ventricle of mice at PD2, and the brain sections were prepared on PD5 and PD9. As previously reported (Peltekian et al., 1997), X-gal staining revealed that the virus infected the brain cells, including OPCs, in the striatum and corpus callosum adjacent to the dorsolateral corner of the lateral ventricle. Comparative light microscopic observation of the sections of Ad-β-Gal-injected and untreated hemispheres of the brain showed no apparent morphological differences except for occasional enlargement of the ventrical space as described in Materials and Methods. Immunohistochemistry using anti-MAG and anti-MBP antibodies showed essentially the same distribution and intensity of immunostaining of these molecules, suggesting little or no effect of the virus injection itself on the development of oligodendrocytes (Fig. 3). On the basis of these findings, we injected adenoviral vector encoding shRNA-Ddx54

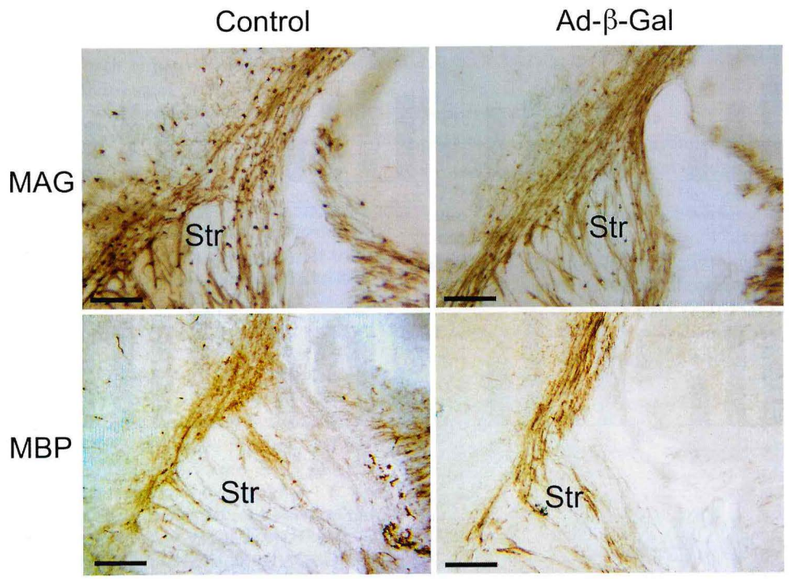

Fig. 3. Immunohistochemistry of Ad-β-Gal-injected brain sections using anti-MAG and anti-MBP antibodies. The sections prepared from the untreated "control" and "Ad-β-Gal"-injected hemispheres of PD9 brains were examined by immunohistochemistry with anti-MAG (upper row) or anti-MBP (lower row) antibodies and visualized with a chromogen, DAB. The immunosignals of MAG and MBP showed essentially a similar distribution in both the control and the Ad-β-Gal sections. Str, striatum. Scale bars = 50 μm.

(Ad-shRNA:Ddx54) into the left lateral ventricle and compared the brain sections of both sides on PD9 by immunohistochemistry with MAG, Olig2, and Camsap1, which are specific markers for mature oligodendrocytes, OPCs, and astrocytic lineage cells, respectively. Immunostaining using chromogenic substrates by anti-MAG antibody demonstrated that a substantial amount of MAG immunosignals was presented in the Ad-shRNA:Ddx54-injected brain. The distribution of MAG-positive cells in the injected side was somewhat similar to that in the untreated cerebral hemisphere, but the pattern of their processes was quite different from that of the control side (Fig. 4). In the untreated cerebral hemisphere, the ovoid and intense filamentous structures of MAG immunosignals presumably represented cell bodies and myelinated axons, respectively. By contrast, in the Ad-shRNA:Ddx54-injected cerebral hemisphere, a diffuse pattern of fine processes of MAG immunosignals was prominent, with fewer intense filamentous structures. The immunohistochemistry of Olig2 revealed a large number of $Olig2^+$ cells in the control cerebral hemisphere, showing essentially the same pattern as that in the Ad-shRNA:Ddx54-injected side (Fig. 5). Camsap1, which is a highly specific marker of the astrocyte lineage (Yamamoto et al., 2009), showed more intense immunostaining in the injected hemisphere in comparison with that in the control side, although the difference did not reach statistical significance (Fig. 5). These findings indicate that, in Ad-shRNA:Ddx54-infected brain, a substantial amount of MAG^+ mature oligodendrocytes, $Olig2^+$ OPCs, and $Camsap1^+$ astrocyte-lineage cells were present, but their distribution and/or shape, especially those of MAG^+ oligodendrocytes, had changed. To clarify this point, we have performed a double immunostaining of MAG/neurofilament, MBP/neurofilament, and MAG/MBP using fluorescent dye-conjugated secondary antibodies. In the Ddx54-knockdown brain, a large portion of MAG immunosignals was located in the regions containing neurofilament signals corresponding to the axons, but their fine processes were scattered diffusely, apparently independent of the neurofilaments along the axons (Fig. 6). Furthermore, in the Ddx54-knockdown brain, MBP immunosignals accumulated in the subplate layer and did not intrude into corpus callosum, where substantial amounts of neurofilament signals were present (Fig. 7). Double staining of MAG and MBP showed that, in Ddx54-knockdown brain, these two major myelin structural proteins were distributed with less overlap compared with those in the control side (Fig. 8). It was also noted that, in contrast to MBP, MAG immunosignals were present in the corpus callosum.

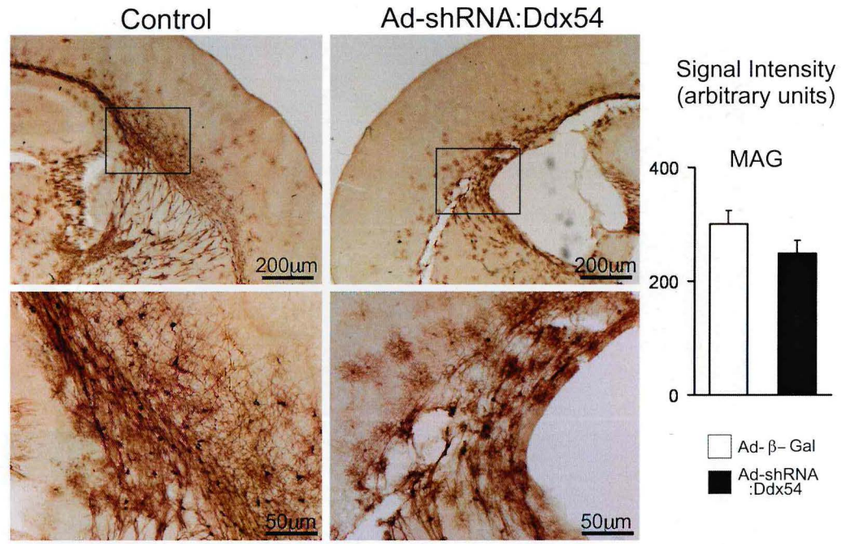

Fig. 4. Immunohistochemistry of Ad-shRNA:Ddx54-injected brain sections using anti-MAG antibody. The sections prepared from the untreated "control" and "Ad-shRNA:Ddx54"-injected hemispheres of PD9 brains were examined by immunohistochemistry with an anti-MAG antibody. In control sections, MAG signals stained the ovoid cell bodies as well as the intense filamentous bundles over the cortical plate, subplate layer, and white matter (corpus callosum). In Ad-shRNA:Ddx54 sections, a diffuse pattern of fine processes of MAG immunosignals was prominent, with fewer intense filamentous structures. The intensity of MAG immunosignal was measured by image analysis. Data represent mean ± SEM (n = 3).

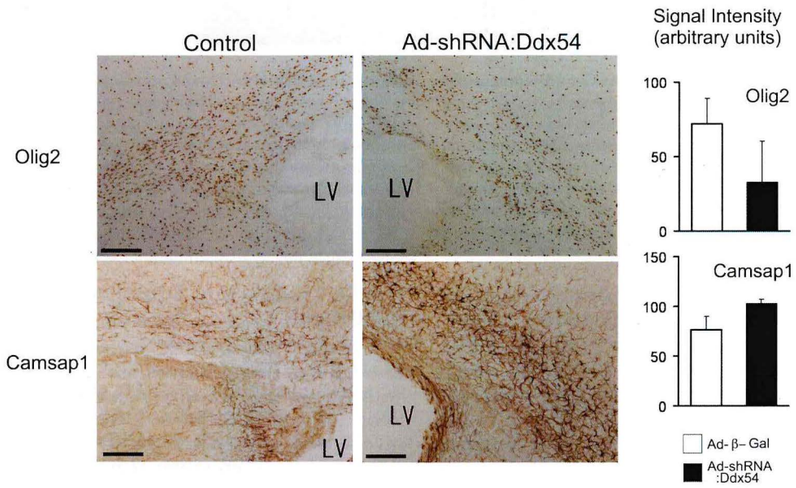

Fig. 5. Immunohistochemistry of Ad-shRNA:Ddx54-injected brain sections using anti-Olig2 and A3B10 antibodies. The sections prepared from the untreated "control" and "Ad-shRNA:Ddx54"-injected hemispheres of PD9 brains were examined by immunohistochemistry with anti-Olig2 (upper row) or A3B10 (lower row) antibodies and visualized with a chromogen, DAB. The immunosignals of Olig2 showed a similar distribution in both the control and the Ad-shRNA:Ddx54 sections, although the staining against Camsap1 (using A3B10) was somewhat more intense in the Ddx54-knockdown left brain. LV, lateral ventricle. The intensity of immunosignals was measured by image analysis. Data represent mean ± SEM (n = 3). Scale bars = 50 μm.

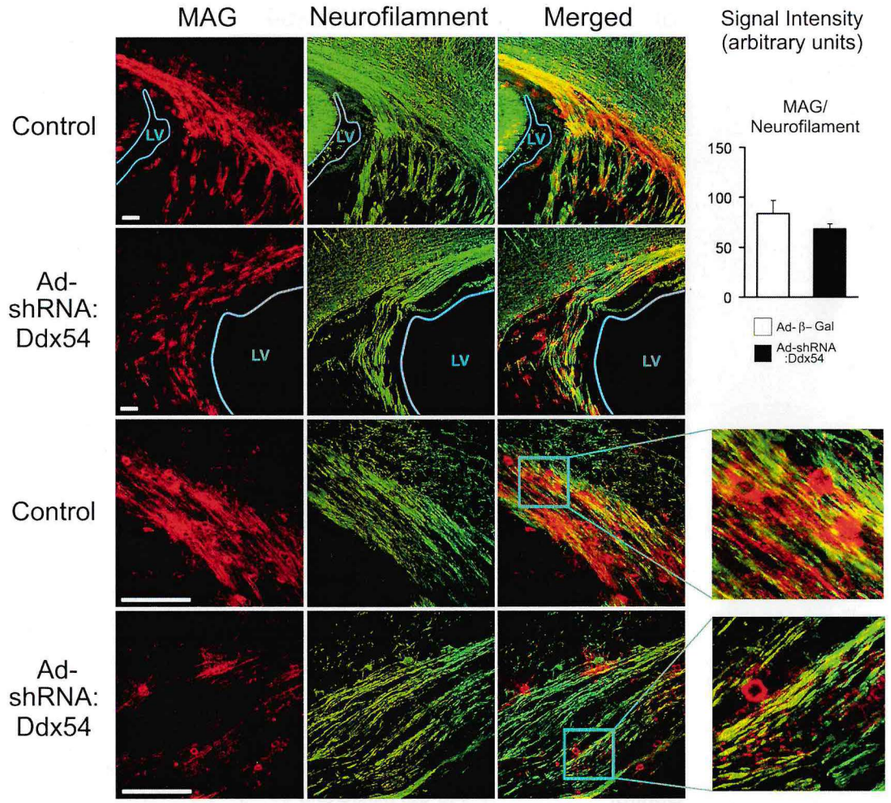

Fig. 6. Double immunostaining using anti-MAG and antineurofilament antibodies. The sections prepared from the untreated "control" and "Ad-shRNA:Ddx54"-injected hemispheres of PD9 brains were examined by immunohistochemistry with anti-MAG and anti-neurofilament (RT97) antibodies. In the control sections, MAG immunosignals generated a "cell body" shape as well as a "filamentous" shape. The intensity of the filamentous pattern of staining was codistributed with RT97 immunosignals, which correspond to axons. In Ad-shRNA:Ddx54 sections, "filamentous" immunosignals of MAG were observed only in very small amounts. Immunosignals of RT97 were essentially identical between control and Ad-shRNA:Ddx54 brain sections. LV, lateral ventricle. The intensity of immunosignals was measured by image analysis. The ratio of MAG to neurofilament was calculated. Data represent mean ± SEM (n = 3). Scale bars = 100 μm.

Immunoblot Analysis of Oligodendrocyte-Specific Proteins

To investigate further the effect of Ddx54 knockdown, we analyzed oligodendrocyte- and myelin-specific proteins by immunoblot on brain homogenates prepared from control vector- and Ddx54 knockdown vector-treated mice (Fig. 9). There was no apparent difference in most of the proteins tested, that is, MAG; three isoforms (14, 17.5, and 18 kDa) of MBP; 2′,3′-cyclic nucleotide 3′ phosphodiesterase (CNPase); Sox10; and QKI-5, −6, and −7 proteins. However, the level of Ddx54 protein decreased, indicating the efficient silencing occurred by Ad-shRNA:Ddx54 treatment. Only the level of the 21.5-kDa MBP isoform decreased in Ddx54-knockdown brain.

Ddx54 Transfection Stimulates Transcription of MBP Gene

Ddx54 is a member of the DEAD-box RNA helicase family. This family of proteins is known to interact with certain mRNA species and regulate their transcription, splicing, decay, and translation. Therefore, we investigated the effect of Ddx54 protein on *Mbp* mRNA. The 5′-promoter region and 5′-promoter + 3′-untranslated region of *Mbp* were fused to the luciferase reporter plasmid, giving pMBP-Luc and pMBP-Luc-3UTR, respectively. These constructs were transfected with *Ddx54*-expressing vector to cultured neuroepithelial cells of embryo. The cotransfected cells were stimulated by estradiol (E2) and dbcAMP plus theophylline, which are known to enhance the oligodendrocyte differentiation, myelination, and MBP expression. As shown in Figure 10, dbcAMP plus theophylline increased the luciferase activity of both pMBP-Luc and pMBP-Luc-3UTR, but E2 showed no effect. *Ddx54* transfection into the control group increased the luciferase activity to a level similar to that induced by dbcAMP plus theophylline. However, the dbcAMP plus theophylline- and E2-treated cells showed no additional effect on *Ddx54* transfection.

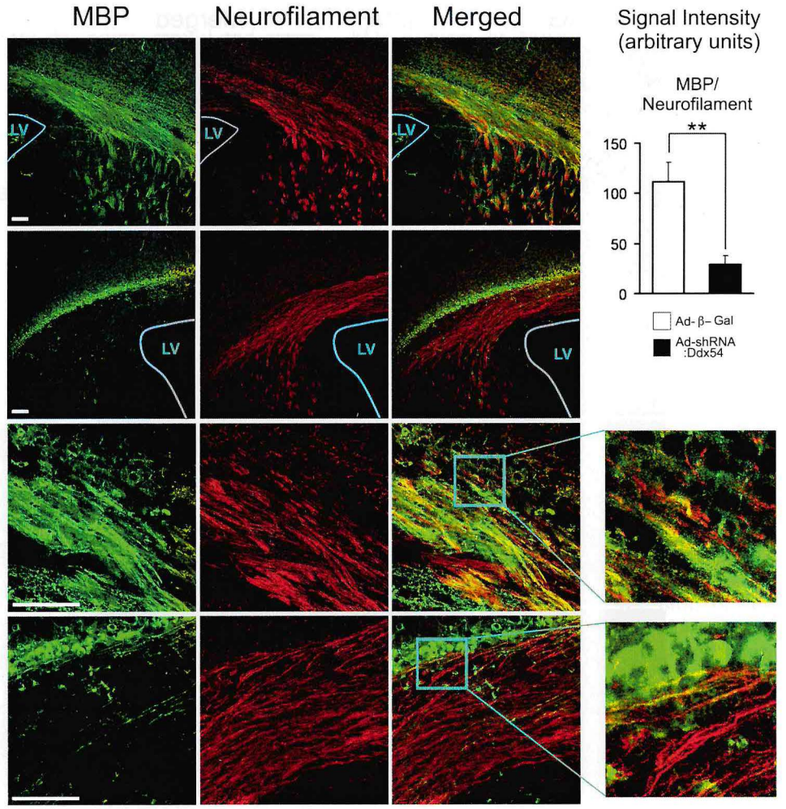

Fig. 7. Double immunostaining using anti-MBP and antineurofilament antibodies. The sections prepared from the untreated "control" and "Ad-shRNA:Ddx54"-injected hemispheres of PD9 brains were examined by immunohistochemistry with anti-MBP and antineurofilament antibodies. In the control sections, MBP immunosignals generated a "cell body" shape as well as a "filamentous" shape. The intensity of the MBP immunosignal was codistributed with neurofilament immunosignals, which correspond to axons. In Ad-shRNA:Ddx54 sections, MBP immunosignals accumulated almost exclusively in the subplate layer, and only trace amounts of MBP immunosignals were observed in white matter (corpus callosum). No colocalization of MBP and neurofilament signals was observed. Immunosignals of neurofilament were essentially identical between control and Ad-shRNA:Ddx54 brain sections. LV, lateral ventricle. The intensity of immunosignals was measured by image analysis. The ratio of MBP to neurofilament was calculated. Data represent mean ± SEM (n = 3). $^{**}P < 0.01$. Scale bars = 100 μm.

Analysis of mRNA Bound to Ddx54 Protein

To clarify whether Ddx54 RNA helicase can bind *Mbp* mRNA, we immunoprecipitated cell lysate prepared from the HEK293 cells cotransfected with the vectors expressing *Ddx54* and *Mbp* genes. PCR amplification of the sequences of mRNA coimmunoprecipitated with Ddx54 protein suggested that all four isoforms of *Mbp* mRNA bind to Ddx54 protein (Fig. 11).

DISCUSSION

In demyelinating diseases, such as multiple sclerosis and progressive multifocal leukoencephalopathy, large numbers of OPCs accumulate in demyelinated lesions (Wolswijk, 1998). However, these cells often fail to differentiate to mature oligodendrocytes and to myelinate axons (Piaton et al., 2009; Watzlawik et al., 2010). Understanding why remyelination fails within demyeli-

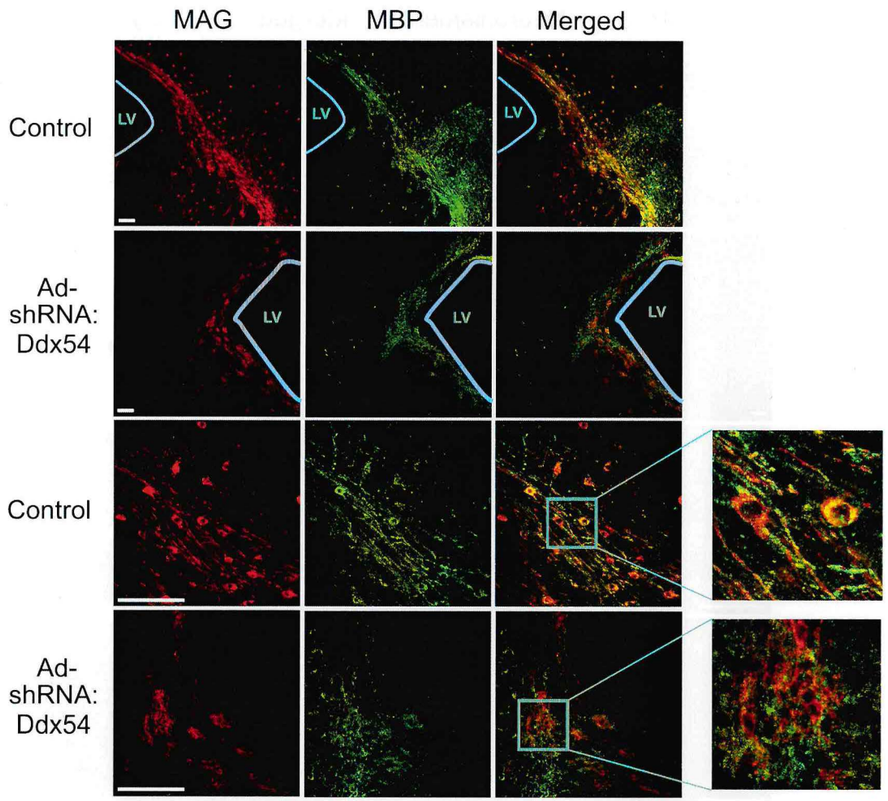

Fig. 8. Double immunostaining using anti-MBP and anti-MAG antibodies. The sections prepared from the untreated "control" and "Ad-shRNA:Ddx54"-injected hemispheres of PD9 brains were examined by immunohistochemistry with anti-MBP and anti-MAG antibodies. In the control sections, both the MBP and the MAG immunosignals generated a "cell body" shape as well as a "filamentous" shape, and the two immunosignals were codistributed. In Ad-shRNA:Ddx54 sections, weak immunosignals of MAG formed a "cell body" shape, but no filamentous signals were observed. Anti-MBP antibody gave even weaker immunosignals. Double staining of MAG and MBP showed that, in Ddx54-knockdown brain, these two major myelin structural proteins were distributed with less of an overlap compared with those of the control side. LV, lateral ventricle. Scale bars = 100 μm.

nated lesions could lead to therapeutic targets for many neurological diseases involving demyelination. Inhibitory molecules on OPC maturation and myelination such as hyarulonan (Back et al., 2005) and bone morphogenic protein (Wang et al., 2011) released from activated astrocytes in demyelinated lesions have been proposed as the mechanism of remyelination failure. Approaches aiming at the enhancement of intrinsic repair mechanisms by regulation of estrogen receptor β (Crawford et al., 2010), Notch1 (Zhang et al., 2009), Wnt-β-catenin (Fancy et al., 2009), Fyn-RhoA (Baer et al., 2009), and LINGO-1 (Mi et al., 2009) signalings have also been addressed. However, to develop potential therapeutic strategies for CNS demyelination, it will be essential to resolve better the mechanisms by which oligodendrocytes interpret and translate extrinsic signals into the initiation of myelination.

In the present study, knockdown of Ddx54 resulted in remarkable aberrations in the distribution of MBP and MAG proteins, which are specific markers for mature oligodendrocytes as well as the essential structural proteins for compacted myelin. The prominent decrease in filamentous shape in MAG immunosignals and the extensive lack of those of MBP in corpus callosum, suggest that normal myelination may not occur in Ddx54 knocked down brains. Because the differentiation and maturation of oligodendrocytes may proceed to the terminal stage (whose hallmark is thought to be the expression of myelin-specific genes such as MBP and MAG), this aberration suggests that additional, unknown molecular players may be required in the final stage of the myelination process and that therapeutic approaches aimed at the promotion of differentiation and maturation of oligodendrocytes might still be insufficient to complete the formation of myelin sheath wrapping around axons. However, to clarify this point, careful and extensive investigation of the time course of formation of myelin sheath, including electron microscopic examination, must be performed.

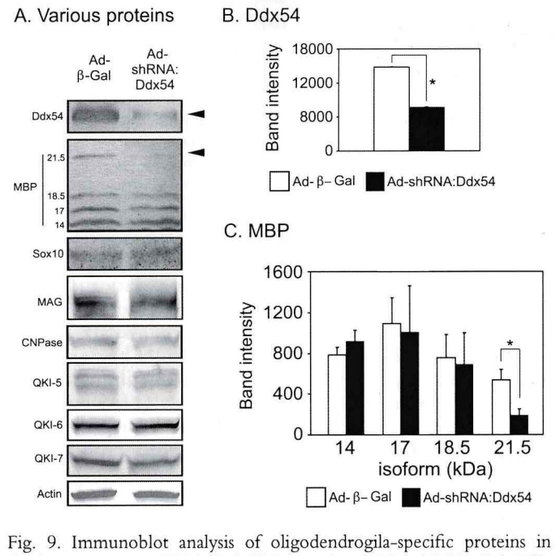

Fig. 9. Immunoblot analysis of oligodendrogila-specific proteins in the homogenates of "Ad-β-Gal"-injected and "Ad-shRNA:Ddx54"-injected brains. The homogenates were prepared from Ad-β-Gal-injected and Ad-shRNA:Ddx54-injected PD9 brains. The proteins in the homogenates were resolved by electrophoresis, blotted, and detected by the antibodies indicated. **A:** Representative images. **B:** Quantitative data for Ddx54 protein. **C:** Quantitative data for four MBP isoforms are shown. For quantitation, three mice per group were used. Data represent mean ± SD. $*P < 0.05$.

One candidate for such a player may be the 21.5-kDa isoform of MBP. MBP binds to the cytoplasmic surfaces of the membrane and brings them close together so that myelin can form a tight spiral around the axon. MBP is, therefore, an indispensable structural component for myelin sheath formation. However, the present data clearly indicate that the mere presence of MBP proteins is insufficient to complete the process of myelin compaction. Similar findings have been obtained in the demyelinated brain tissue from aged rodents, cuprizone-treated mice, and FcR-γ/Fyn double-knockout mice. These brain tissues contained a substantial amount of MBP even in demyelinated regions. However, the 21.5-kDa isoform of MBP, especially the phosphorylated species, specifically diminished in the demyelinated regions of the brain. Remyelination triggered by certain neuroprotective drugs and/or withdrawal of cuprizone were accompanied by the recovery of the 21.5-kDa MBP. The 21.5- and 17-kDa MBP isoforms contain exon II region and have been reported to be translocated into the nucleus in a phosphorylation-dependent manner, whereas the two other MBP isoforms are not transported to the nucleus (Pedraza, 1997; Pedraza et al., 1997; Boggs, 2006). These reports suggest that exon II-containing MBPs may play additional roles in myelination, that is, the regulation of expression of certain genes as the signaling molecules. The disappearance of 21.5-kDa MBP from demyelinated brain tissue may indicate a loss of the regulatory action of the isoform in terms of myelin sheath formation.

It must also be noted that the forced expression of the Ddx54 gene with MBP genes in HEK293 cells resulted in the enhanced nuclear transport of the 21.5-kDa MBP isoform (Ueki et al., 2012). Furthermore, our previous study has also shown that Ddx54 protein interacts with all MBP isoforms in situ, i.e., in the brain and oligodendrocyte culture. Therefore, Ddx54 could directly affect the intracellular localization of MBP. This

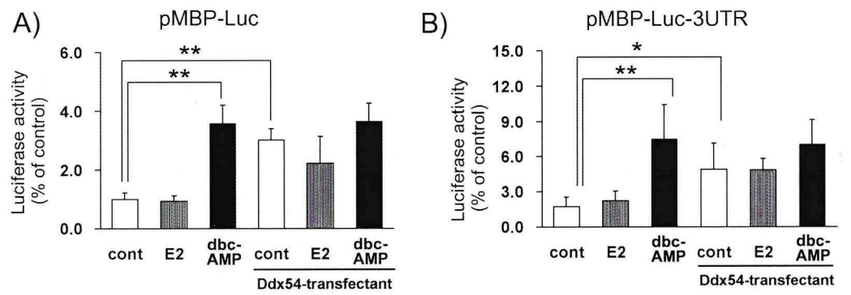

Fig. 10. Effect of Ddx54 expression on the MBP promoter-mediated luciferase activity. E14 neuroepithelial cells were transfected with pMBP-Luc (**A**) and pMBP-Luc-3UTR (**B**). Luciferase activity of both plasmids was increased with 24-hr treatment with dibutyryl cAMP (dbcAMP) + theophylline, but not estradiol (E2). Cotransfection of Ddx54-expressing gene also enhanced the activity of both plasmids. However, cotransfection did not alter the effect of E2 and dbcAMP on luciferase activity. Data represent mean ± SD. $*P < 0.05$, $**P < 0.01$.

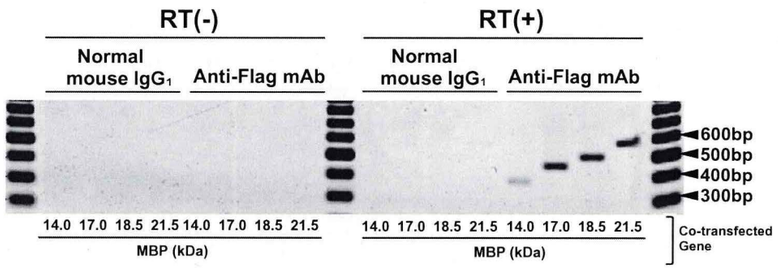

Fig. 11. Identification of mRNA bound to Ddx54 protein. The expression plasmids encoding Ddx54/Flag tag and each of four isoforms of MBP/Myc tag were cotransfected into HEK 293 cells. Ddx54 protein was immunoprecipitated with anti-Flag tag antibody, and the RNA extracted from the precipitate was analyzed by RT-PCR using an MBP-specific primer. A scanned image of the agarose gel electrophoresis is shown. The immunoprecipitates prepared by anti-Flag tag antibody were found to contain all four isoforms of *Mbp* mRNA, whereas the precipitates prepared by control IgG were not. In all cases, omission of reverse transcriptase from the reaction mix resulted in no amplification product. RT(−), reverse transcriptase omitted; RT(+), reverse transcriptase included.

seems to be in good accordance with the marked difference in MBP distribution in Ddx54-knockdown brain as demonstrated in the present study. In the normal developmental process of human and rodent brains, most late OPCs (as marked by the presence of O4 antigens) are found in the subplate layer. OPCs subsequently transform to premyelinating $O1^+$ oligodendrocytes and then into mature oligodendrocytes ready to myelinate axons. During this process, myelin proteins, such as MBP and phospholipid protein, start to be expressed in cell bodies and thereafter shift their expression to processes that form myelin sheaths (Jakovcevski and Zecevic, 2005). Although mature oligodendrocytes are distributed in both subplate layer and emerging white matter, the oligodendrocytes expressing MBP in processes are located predominantly in corpus callosum. The immunohistochemical staining of MBP in untreated P9 brain shown in Figure 6 is in good accordance with the above-mentioned picture of developmental biology. Surprisingly, however, MBP immunosignals in Ddx54-knockdown brain were confined to the subplate layer and were not detected in the white matter. This suggests that Ddx54 protein may be essential 1) to transfer MBP from the cell body to processes and/or 2) to make oligodendrocytes migrate from the subplate layer to corpus callosum. Corpus callosum is the major site of myelination, where processes elongated from the cell body of oligodendrocytes and nerve fibers meet to form a myelin sheath. MBP is the indispensable protein for wrapping and compaction of myelin sheath. Therefore, the extensive lack of MBP would prevent oligodendrocytes from forming the myelin sheath around the axons. Because MAG immunosignals were detected in corpus callosum, it is implausible that no process elongates and intrudes into this locus. Therefore, the lack of MBP in corpus callosum appears to be related to its impotence in transporting MBP from the cell body to the tip of the processes.

Our previous investigation suggests the association between Ddx54 protein and MBP isoforms, and the present study addresses the possible association between Ddx54 protein and *Mbp* mRNAs. Transfection of the *Ddx54* gene activated transcription of MBP reporter plasmids, which encoded the 5′ promoter region and 3′ untranslated region of *Mbp*. The results of immunoprecipitation experiments that analyzed mRNA bound to Ddx54 protein strongly suggest that Ddx54 protein may associate directly with *Mbp* mRNA. Ddx54 is a member of the DEAD-box RNA helicase family of enzymes, which are present in all eukaryotic cells. These highly conserved enzymes are required for nearly all aspects of RNA metabolism, from transcription and translation to mRNA decay (Linder and Jankowsky, 2011). The proteins generally function as part of larger multicomponent assemblies, such as the spliceosome or the eukaryotic translation initiation machinery (Jarmoskaite and Russell, 2011). Although all DEAD-box proteins contain a structurally highly conserved core with conserved ATP-binding and RNA-binding sites, different proteins have been associated with diverse and seemingly unrelated functions, including the disassembly of RNPs, chaperoning during RNA folding, and stabilization of protein complexes on RNA (Cordin et al., 2006; Jarmoskaite and Russell, 2011). Ddx54 is known to bind to 14-4-3 protein (Satoh et al., 2006) and estrogen receptors (Rajendran et al., 2003). However, the biological activity of this protein is largely unknown. Nonetheless, structural, biophysical, biochemical, and genetic research on this family of proteins suggests that Ddx54 protein plays an important role in ribosome biogenesis (Linder and Jankowsky, 2011). The major activity of DEAD-box helicases is the displacement of the target protein from RNA. Ddx54 protein interacts with both MBP and its cognate mRNA. This observation suggests that Ddx54 could directly regulate the biosynthesis of MBP at the intersection of MBP mRNAs, isoform proteins, and their synthesizing machinery, ribosomes. The biosynthesis of MBP is known to occur in the actual loci, i.e., on free polysomes at myelinating cellular processes, as well as in the cell body. The lack of MBP in corpus callosum

may be related to its dysregulation of transport of MBP mRNA in Ddx54-knockdown brains. Thus Ddx54 protein might mediate every aspect of MBP biology, namely, transcription, splicing, translation, transport, and decay of mRNA and protein.

As described above, Ddx54 appears to have a particular relationship with MBP via direct interaction with its mRNA and protein. However, immunohistochemistry of MAG (but not of Olig2) was also profoundly changed by injection of Ad-shRNA:Ddx54 vector (Fig. 4). Furthermore, Ddx54 knockdown in OPC resulted in decreased mRNA expression of Mag and Plp, suggesting that Ddx54 might play an important role in a wide array of mRNA/protein expression during the differentiation process of oligodendrocytes (Fig. 2). As we have previously reported, Ddx54 is detected from a very early stage of neural development to the aged rats. Accordingly, by using in vitro OPC/oligodendrocyte cultures, we have observed that Ddx54 protein is expressed in early OPC and that its localization changes dynamically with progression of the differentiation process even before the commencement of MBP expression (unpublished data). These data strongly suggest that Ddx54 may play a role not only in MBP regulation but also in a wide range of OPC/oligodendrocyte biology. Along these lines, possible effects of the protein on proliferation and cell death of oligodendrocyte-lineage cells should be analyzed with particular attention. We intend to perform extensive studies in the future to clarify this point. In addition, an investigation of tissue and subcellular localization of Ddx54 mRNA and protein during development from the embryo through the adult stages, especially in mice, should be performed. The knockdown strategy of Ddx54 protein via injection of Ad-shRNA:Ddx54 vector into the brains at various developmental stages will contribute to elucidation of the physiological (and presumably pathological) significance of this protein. Because the use of adenovirus vector has its own limitations, such as a short span of expression, cellular toxicity, and tropism for mature cells, the use of alternative technologies (e.g., lentivirus vectors) may also be considered in future studies.

In summary, we have shown that Ddx54 protein plays an extraordinarily important role in MBP biology and CNS myelination. The present study, as far as we know, is the first report indicating the possible physiological function of Ddx54 protein. Because Ddx54 is expressed in oligodendroglial-lineage cells throughout the earliest stages of development to old age, the present findings presumably provide only one aspect of the wide spectrum of biological activities mediated by Ddx54. The elucidation of the biological role of Ddx54 in oligodendroglial-lineage cells will deepen our understanding of myelin biology and open the way to the development of novel therapeutic strategies for demyelinating diseases.

REFERENCES

Akiyama K, Ichinose S, Omori A, Sakurai Y, Asou H. 2002. Study of expression of myelin basic proteins (MBPs) in developing rat brain using a novel antibody reacting with four major isoforms of MBP. J Neurosci Res 68:19–28.

Alexander HK, Booy EP, Xiao W, Ezzati P, Baust H, Los M. 2007. Selected technologies to control genes and their products for experimental and clinical purposes. Arch Immunol Ther Exp 55:139–149.

Back SA, Tuohy TM, Chen H, Wallingford N, Craig A, Struve J, Luo NL, Banine F, Liu Y, Chang A, Trapp BD, Bebo BF Jr, Rao MS, Sherman LS. 2005. Hyaluronan accumulates in demyelinated lesions and inhibits oligodendrocyte progenitor maturation. Nat Med 11:966–972.

Baer AS, Syed YA, Kang SU, Mitteregger D, Vig R, Ffrench-Constant C, Franklin RJ, Altmann F, Lubec G, Kotter MR. 2009. Myelin-mediated inhibition of oligodendrocyte precursor differentiation can be overcome by pharmacological modulation of Fyn-RhoA and protein kinase C signalling. Brain 132:465–481.

Boggs JM. 2006. Myelin basic protein: a multifunctional protein. Cell Mol Life Sci 63:1945–1961.

Cordin O, Banroques J, Tanner NK, Linder P. 2006. The DEAD-box protein family of RNA helicases. Gene 367:17–37.

Crawford DK, Mangiardi M, Song B, Patel R, Du S, Sofroniew MV, Voskuhl RR, Tiwari-Woodruff SK. 2010. Oestrogen receptor beta ligand: a novel treatment to enhance endogenous functional remyelination. Brain 133:2999–3016.

Dugas JC, Ibrahim A, Barres BA. 2007. A crucial role for p57(Kip2) in the intracellular timer that controls oligodendrocyte differentiation. J Neurosci 27:6185–6196.

Fancy SP, Baranzini SE, Zhao C, Yuk DI, Irvine KA, Kaing S, Sanai N, Franklin RJ, Rowitch DH. 2009. Dysregulation of the Wnt pathway inhibits timely myelination and remyelination in the mammalian CNS. Genes Dev 23:1571–1585.

Goldman JE. 1995. Lineage, migration, and fate determination of postnatal subventricular zone cells in the mammalian CNS. J Neurooncol 24:61–64.

Imada S, Yamamoto M, Tanaka K, Seiwa C, Watanabe K, Kamei Y, Kozuma S, Taketani Y, Asou H. 2010. Hypothermia-induced increase of oligodendrocyte precursor cells: possible involvement of plasmalemmal voltage-dependent anion channel 1. J Neurosci Res 88:3457–3466.

Jakovcevski I, Zecevic N. 2005. Sequence of oligodendrocyte development in the human fetal telencephalon. Glia 49:480–491.

Jarmoskaite I, Russell R. 2011. DEAD-box proteins as RNA helicases and chaperones. Wiley Interdiscip Rev RNA 2:135–152.

Linder P, Jankowsky E. 2011. From unwinding to clamping—the DEAD box RNA helicase family. Nat Rev Mol Cell Biol 12:505–516.

Mi S, Miller RH, Tang W, Lee X, Hu B, Wu W, Zhang Y, Shields CB, Zhang Y, Miklasz S, Shea D, Mason J, Franklin RJ, Ji B, Shao Z, Chedotal A, Bernard F, Roulois A, Xu J, Jung V, Pepinsky B. 2009. Promotion of central nervous system remyelination by induced differentiation of oligodendrocyte precursor cells. Ann Neurol 65:304–315.

Miura M, Tamura T, Aoyama A, Mikoshiba K. 1989. The promoter elements of the mouse myelin basic protein gene function efficiently in NG108–15 neuronal/glial cells. Gene 75:31–38.

Nakashima K, Yanagisawa M, Arakawa H, Kimura N, Hisatsune T, Kawabata M, Miyazono K, Taga T. 1999. Synergistic signaling in fetal brain by STAT3-Smad1 complex bridged by p300. Science 284:479–482.

Pedraza L. 1997. Nuclear transport of myelin basic protein. J Neurosci Res 50:258–264.

Pedraza L, Fidler L, Staugaitis SM, Colman DR. 1997. The active transport of myelin basic protein into the nucleus suggests a regulatory role in myelination. Neuron 18:579–589.

Peltekian E, Parrish E, Bouchard C, Peschanski M, Lisovoski F. 1997. Adenovirus-mediated gene transfer to the brain: methodological assessment. J Neurosci Methods 71:77–84.

Pfeiffer SE, Warrington AE, Bansal R. 1993. The oligodendrocyte and its many cellular processes. Trends Cell Biol 3:191–197.

Piaton G, Williams A, Seilhean D, Lubetzki C. 2009. Remyelination in multiple sclerosis. Prog Brain Res 175:453–464.

Rajendran RR, Nye AC, Frasor J, Balsara RD, Martini PG, Katzenellenbogen BS. 2003. Regulation of nuclear receptor transcriptional activity by a novel DEAD box RNA helicase (DP97). J Biol Chem 278:4628–4638.

Satoh J, Nanri Y, Yamamura T. 2006. Rapid identification of 14-3-3-binding proteins by protein microarray analysis. J Neurosci Methods 152:278–288.

Ueki T, Tsuruo Y, Yamamoto Y, Yoshimura K, Takanaga H, Seiwa C, Motojima K, Asou H, Yamamoto M. 2012. A new monoclonal antibody, 4F2, specific for the oligodendroglial cell lineage, recognizes ATP-dependent RNA helicase Ddx54: possible association with myelin basic protein. J Neurosci Res 90:48–59.

Wang Y, Cheng X, He Q, Zheng Y, Kim DH, Whittemore SR, Cao QL. 2011. Astrocytes from the contused spinal cord inhibit oligodendrocyte differentiation of adult oligodendrocyte precursor cells by increasing the expression of bone morphogenetic proteins. J Neurosci 31:6053–6058.

Watzlawik J, Warrington AE, Rodriguez M. 2010. Importance of oligodendrocyte protection, BBB breakdown and inflammation for remyelination. Expert Rev Neurother 10:441–457.

Wolswijk G. 1998. Chronic stage multiple sclerosis lesions contain a relatively quiescent population of oligodendrocyte precursor cells. J Neurosci 18:601–609.

Yamamoto M, Yoshimura K, Kitada M, Nakahara J, Seiwa C, Ueki T, Shimoda Y, Ishige A, Watanabe K, Asou H. 2009. A new monoclonal antibody, A3B10, specific for astrocyte-lineage cells recognizes calmodulin-regulated spectrin-associated protein 1 (Camsap1). J Neurosci Res 87:503–513.

Yoshioka N, Hisanaga S, Kawano H. 2010. Suppression of fibrotic scar formation promotes axonal regeneration without disturbing blood–brain barrier repair and withdrawal of leukocytes after traumatic brain injury. J Comp Neurol 518:3867–3881.

Yoshioka N, Asou H, Hisanaga SI, Kawano H. 2011a. The astrocytic lineage marker calmodulin-regulated spectrin-associated protein 1 (camsap1): phenotypic heterogeneity of newly born camsap1-expressing cells in injured mouse brain. J Comp Neurol (in press).

Yoshioka N, Kimura-Kuroda J, Saito T, Kawamura K, Hisanaga S, Kawano H. 2011b. Small molecule inhibitor of type I transforming growth factor-beta receptor kinase ameliorates the inhibitory milieu in injured brain and promotes regeneration of nigrostriatal dopaminergic axons. J Neurosci Res 89:381–393.

Zhang Y, Argaw AT, Gurfein BT, Zameer A, Snyder BJ, Ge C, Lu QR, Rowitch DH, Raine CS, Brosnan CF, John GR. 2009. Notch1 signaling plays a role in regulating precursor differentiation during CNS remyelination. Proc Natl Acad Sci U S A 106:19162–19167.